

Collective Modes in Light Nuclei from First Principles

T. Dytrych,¹ K. D. Launey,¹ J. P. Draayer,¹ P. Maris,² J. P. Vary,² E. Saule,³ U. Catalyurek,^{3,4} M. Sosonkina,⁵ D. Langr,⁶ and M. A. Caprio⁷

¹*Department of Physics and Astronomy, Louisiana State University, Baton Rouge, LA 70803, USA*

²*Department of Physics and Astronomy, Iowa State University, Ames, IA 50011, USA*

³*Department of Biomedical Informatics, The Ohio State University, Columbus, OH 43210, USA*

⁴*Department of Electrical and Computer Engineering,
The Ohio State University, Columbus, OH 43210, USA*

⁵*Department of Modeling, Simulation and Visualization Engineering,
Old Dominion University, Norfolk, VA 23529, USA*

⁶*Department of Computer Systems, Czech Technical University in Prague, Prague, Czech Republic*

⁷*Department of Physics, University of Notre Dame, Notre Dame, IN 46556, USA*

Results for *ab initio* no-core shell model calculations in a symmetry-adapted SU(3)-based coupling scheme demonstrate that collective modes in light nuclei emerge from first principles. The low-lying states of ⁶Li, ⁸Be, and ⁶He are shown to exhibit orderly patterns that favor spatial configurations with strong quadrupole deformation and complementary low intrinsic spin values, a picture that is consistent with the nuclear symplectic model. The results also suggest a pragmatic path forward to accommodate deformation-driven collective features in *ab initio* analyses when they dominate the nuclear landscape.

Introduction. – Major progress in the development of realistic inter-nucleon interactions along with the utilization of massively parallel computing resources [1–3] have placed *ab initio* approaches [4–14] at the frontier of nuclear structure explorations. The ultimate goal of *ab initio* studies is to establish a link between underlying principles of quantum chromodynamics (quark/gluon considerations) and observed properties of atomic nuclei, including their structure and related reactions. The predictive potential that *ab initio* models hold [15, 16] makes them suitable for targeting short-lived nuclei that are inaccessible by experiment but essential to modeling, for example, of the dynamics of X-ray bursts and the path of nucleosynthesis (see, e.g., [17, 18]).

In this letter, we report on *ab initio* symmetry-adapted no-core shell model (SA-NCSM) results for the ⁶Li (odd-odd), ⁸Be (even-even), and ⁶He (halo) nuclei, using two realistic nucleon-nucleon (*NN*) interactions, the JISP16 [19] and chiral N³LO [20] potentials. The SA-NCSM framework exposes a remarkably simple physical feature that is typically masked in other *ab initio* approaches; the emergence, without *a priori* constraints, of simple orderly patterns that favor spatial configurations with strong quadrupole deformation and low intrinsic spin values. This feature, once exposed and understood, can be used to guide a truncation and augmentation of model spaces to ensure that important properties of atomic nuclei, like enhanced *B(E2)* strengths, nucleon cluster substructures, and others important in reactions, are appropriately accommodated in future *ab initio* studies.

The SA-NCSM joins a no-core shell model (NCSM) theory [4] with a multi-shell, SU(3)-based coupling scheme [21, 22]. Specifically, nuclear wavefunctions are represented as a superposition of many-particle configurations

carrying a particular intrinsic quadrupole deformation linked to the irreducible representation (irrep) labels ($\lambda\mu$) of SU(3) [23–25], and specific intrinsic spins ($S_p S_n S$) for protons, neutrons, and total spin, respectively (proton-neutron formalism). The fact that SU(3) plays a key role, e.g., in the microscopic description of the experimentally observed collectivity of *ds*-shell nuclei [26–30], and for heavy deformed systems [31], tracks from the seminal work of Elliott [21] and is reinforced by the fact that it is the underpinning symmetry of the microscopic symplectic model [32, 33], which provides a comprehensive theoretical foundation for understanding the dominant symmetries of nuclear collective motion [29, 34].

The outcome further suggests a symmetry-guided basis selection that yields results that are nearly indistinguishable from the complete basis counterparts. This is illustrated for ⁶Li and ⁶He for a range of harmonic oscillator (HO) energies $\hbar\Omega$, and $N_{\max}=12$ model spaces, where N_{\max} is the maximum number of HO quanta included in the basis states above the Pauli allowed minimum for a given nucleus. An overarching long-term objective is to extend the reach of the standard NCSM scheme by exploiting symmetry-guided principles that enable one to include configurations beyond the N_{\max} cutoff, while capturing the essence of long-range correlations that often dominate the nuclear landscape.

***Ab initio* realization of collective modes.** – The expansion of eigenstates in the physically relevant SU(3) basis unveils salient features that emerge from the complex dynamics of these strongly interacting many-particle systems. To explore the nature of the most important correlations, we analyze the probability distribution across ($S_p S_n S$) and ($\lambda\mu$) configurations of the four lowest-lying isospin-zero ($T = 0$) states of ⁶Li (1_{gs}^+ , 3_1^+ ,

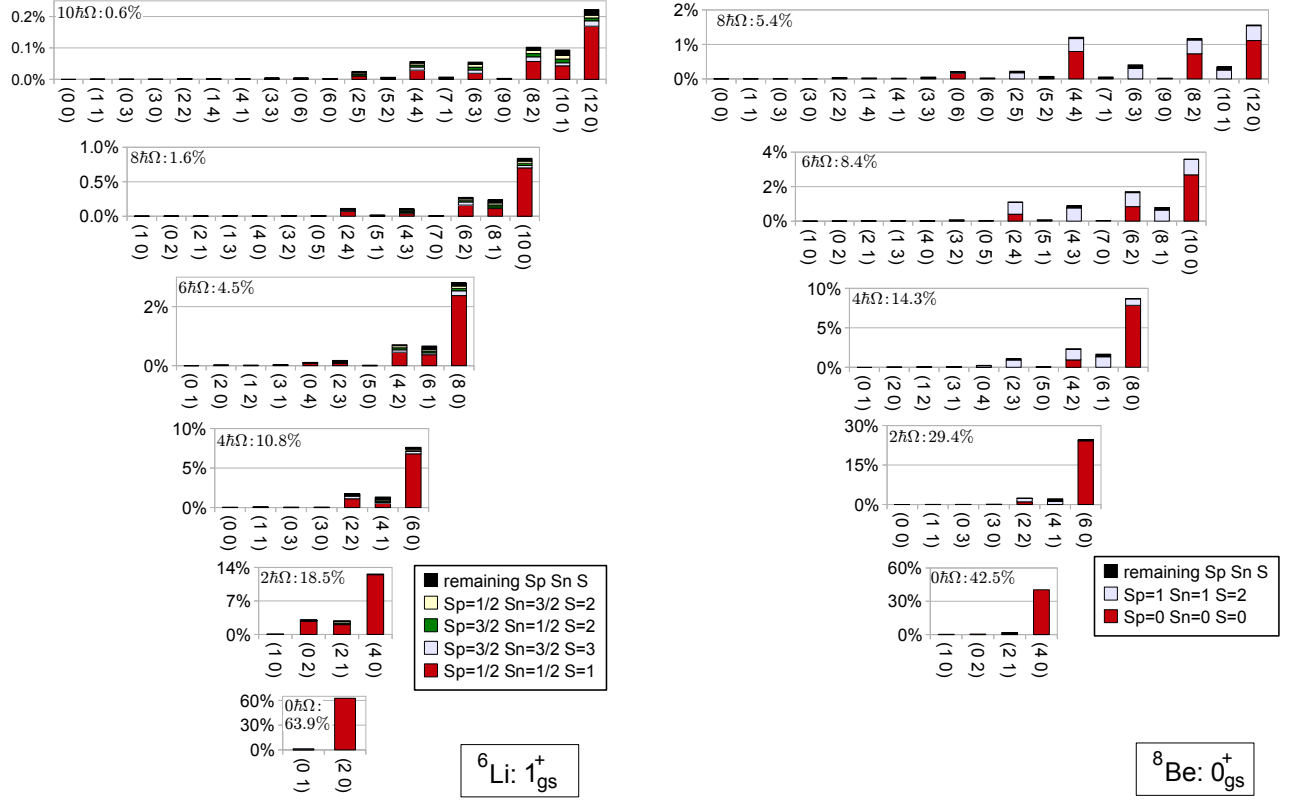


FIG. 1: Probability distributions across $(S_p S_n S)$ and $(\lambda \mu)$ values (horizontal axis) for the calculated 1_{gs}^+ of ${}^6\text{Li}$ obtained for $N_{\text{max}} = 10$ and $\hbar\Omega = 20$ MeV with the JISP16 interaction (left) and the 0_{gs}^+ of ${}^8\text{Be}$ obtained for $N_{\text{max}} = 8$ and $\hbar\Omega = 25$ MeV with the chiral N^3LO interaction (right). The total probability for each $N\hbar\Omega$ subspace is given in the upper left-hand corner of each histogram. The concentration of strengths to the far right demonstrates the dominance of collectivity.

2_1^+ , and 1_2^+), along with the ground-state rotational bands of ${}^8\text{Be}$ and ${}^6\text{He}$. Results for the ground-state of ${}^6\text{Li}$ and ${}^8\text{Be}$, obtained with the JISP16 and chiral N^3LO interactions, respectively, are shown in Figure 1. This figure illustrates a feature common to all the low-energy solutions considered; namely, a highly structured and regular mix of intrinsic spins and $\text{SU}(3)$ spatial quantum numbers that has heretofore gone unrecognized in other *ab initio* studies, and which does not seem to depend on the particular choice of realistic NN potential.

First, consider the spin content. The calculated eigenstates project at a 99% level onto a comparatively small subset of intrinsic spin combinations. For instance, the lowest-lying eigenstates in ${}^6\text{Li}$ are almost entirely realized in terms of configurations characterized by the following intrinsic spin $(S_p S_n S)$ triplets: $(\frac{3}{2} \frac{3}{2} 3)$, $(\frac{1}{2} \frac{3}{2} 2)$, $(\frac{3}{2} \frac{1}{2} 2)$, and $(\frac{1}{2} \frac{1}{2} 1)$, with the last one carrying over 90% of each eigenstate. Similarly, the ground-state bands of ${}^8\text{Be}$ and ${}^6\text{He}$ are found to be dominated by configurations carrying total intrinsic spin of the protons and neutrons equal to zero and one, with the largest contributions due to $(S_p S_n S) = (000)$ and (112) configurations.

Second, consider the spatial degrees of freedom. The mixing of $(\lambda \mu)$ quantum numbers exhibits a remarkably

simple pattern. One of its key features is the preponderance of a single $0\hbar\Omega$ $\text{SU}(3)$ irrep. This so-called leading irrep, is characterized by the largest value of the intrinsic quadrupole deformation [23]. For instance, the low-lying states of ${}^6\text{Li}$ project at a 40%-70% level onto the prolate $0\hbar\Omega$ $\text{SU}(3)$ irrep (20) , as illustrated in Fig. 1. For the ground-state band of ${}^8\text{Be}$ and ${}^6\text{He}$, qualitatively similar dominance of the leading $0\hbar\Omega$ $\text{SU}(3)$ irreps is observed. The dominance of the most deformed $0\hbar\Omega$ configuration indicates that the quadrupole-quadrupole interaction of the Elliott $\text{SU}(3)$ model [21] is realized naturally within an *ab initio* framework.

The analysis also reveals that the dominant $\text{SU}(3)$ basis states at each $N\hbar\Omega$ subspace ($N = 0, 2, 4, \dots$) are typically those with $(\lambda \mu)$ quantum numbers given by

$$\lambda + 2\mu = \lambda_0 + 2\mu_0 + N \quad (1)$$

where λ_0 and μ_0 denote labels of the leading $\text{SU}(3)$ irrep in the $0\hbar\Omega$ ($N = 0$) subspace. We conjecture that this regular pattern of $\text{SU}(3)$ quantum numbers reflects the presence of an underlying symplectic $\text{Sp}(3, \mathbb{R})$ symmetry of microscopic nuclear collective motion [32] that governs the low-energy structure of both even-even and odd-odd p -shell nuclei. This can be seen from the fact that $(\lambda \mu)$

configurations that satisfy condition (1) can be determined from the leading $SU(3)$ irrep $(\lambda_0 \mu_0)$ through a successive application of a specific subset of the $Sp(3, \mathbb{R})$ symplectic $2\hbar\Omega$ raising operators. This subset is composed of the three operators, \hat{A}_{zz} , \hat{A}_{zx} , and \hat{A}_{xx} , that distribute two oscillator quanta in z and x directions, but none in y direction, thereby inducing $SU(3)$ configurations with ever-increasing intrinsic quadrupole deformation. These three operators are the generators of the $Sp(2, \mathbb{R}) \subset Sp(3, \mathbb{R})$ subgroup [35], and give rise to deformed shapes that are energetically favored by an attractive quadrupole-quadrupole interaction [34]. This is consistent with our earlier findings of a clear symplectic $Sp(3, \mathbb{R})$ structure with the same pattern (1) in *ab initio* eigensolutions for ^{12}C and ^{16}O [36].

Furthermore, the $N\hbar\Omega$ configurations with $(\lambda_0 + N \mu_0)$, the so-called stretched states, carry a noticeably higher probability than the others. For instance, the $(2 + N 0)$ stretched states contribute at the 85% level to the ground-state of ^6Li , as can be readily seen in Fig. 1. The sequence of the stretched states is formed by consecutive applications of the \hat{A}_{zz} operator, the generator of $Sp(1, \mathbb{R}) \subset Sp(2, \mathbb{R}) \subset Sp(3, \mathbb{R})$ subgroup, over the leading $SU(3)$ irrep. This translates into distributing N oscillator quanta along the direction of the z -axis only and hence rendering the largest possible deformation.

Symmetry-guided framework. – The observed patterns of intrinsic spin and deformation mixing supports the symmetry-guided basis selection philosophy referenced above. Specifically, one can take advantage of dominant symmetries to relax and refine the definition of the SA-NCSM model space, which for the NCSM is fixed by simply specifying the N_{max} cutoff. In particular, SA-NCSM model spaces can be characterized by a pair of numbers, $\langle N_{\text{max}}^\perp \rangle N_{\text{max}}^\top$, which implies inclusion of the complete space up through N_{max}^\perp , and a subset of the complete set of $(\lambda \mu)$ and $(S_p S_n S)$ irreps between N_{max}^\perp and N_{max}^\top . Though not a primary focus of this paper, an ultimate goal is to be able to carry out SA-NCSM investigations in deformed nuclei with N_{max}^\top values that go beyond the highest N_{max} for which complete NCSM results can be provided.

The SA-NCSM concept focuses on retaining the most important configurations that support the strong many-nucleon correlations of a nuclear system using underlying $Sp(1, \mathbb{R}) \subset Sp(2, \mathbb{R}) \subset Sp(3, \mathbb{R})$ symmetry considerations. It is important to note that for model spaces truncated according to $(\lambda \mu)$ and $(S_p S_n S)$ irreps, the spurious center-of-mass motion can be factored out exactly [37], which represents an important advantage of this scheme.

The efficacy of the symmetry-guided concept is illustrated for SA-NCSM results obtained in model spaces which are expanded beyond a complete N_{max}^\perp space with irreps that span a relatively few dominant intrinsic spin components and carry quadrupole deformation specified by (1). Specifically, we vary N_{max}^\perp from 2 to 10 with

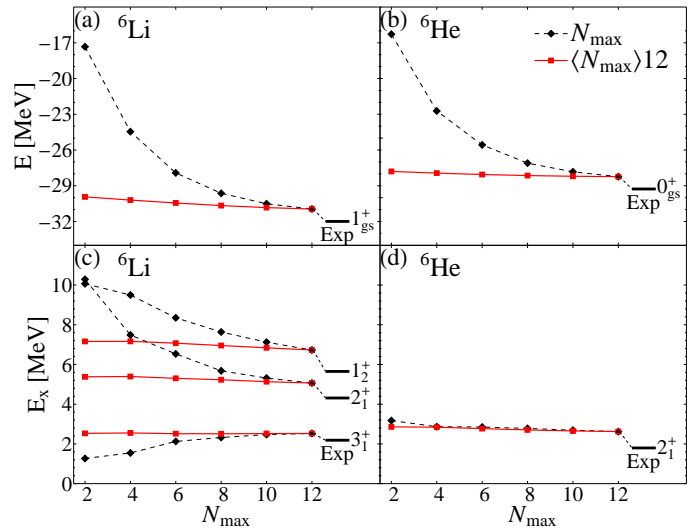


FIG. 2: The ground-state binding energies of ^6Li (a) and ^6He (b), excitation energies of $T = 0$ states of ^6Li (c), 2_1^+ excited state of ^6He (d), shown for the complete N_{max} (dashed black curves) and truncated $\langle N_{\text{max}}^\perp = N_{\text{max}}^\top \rangle 12$ (solid red lines) model spaces. Results shown are for JISP16 and $\hbar\Omega = 20$ MeV. Note the relatively large changes when the complete space is increased from $N_{\text{max}} = 2$ to $N_{\text{max}} = 12$ as compared to nearly constant $\langle N_{\text{max}}^\perp \rangle 12$ SA-NCSM outcomes.

only the subspaces determined by (1) included beyond N_{max}^\perp . This allows us to study convergence of spectroscopic properties towards results obtained in the complete $N_{\text{max}} = 12$ space and hence, probes the efficacy of the SA-NCSM symmetry-guided model space selection concept. In the present study, a Coulomb plus JISP16 NN interaction for $\hbar\Omega$ values ranging from 17.5 up to 25 MeV is used, along with the Gloeckner-Lawson prescription [38] for elimination of spurious center-of-mass excitations. SA-NCSM eigenstates are used to determine spectroscopic properties of low-lying $T = 0$ states of ^6Li and the ground-state band of ^6He for $\langle N_{\text{max}}^\perp \rangle 12$ model spaces.

The results indicate that the observables obtained in the $\langle N_{\text{max}}^\perp \rangle 12$ symmetry-guided truncated spaces are excellent approximations to the corresponding $N_{\text{max}} = 12$ complete-space counterparts. Furthermore, the level of agreement achieved is only marginally dependent on N_{max}^\perp . In particular, the ground-state binding energies obtained in a $\langle 2 \rangle 12$ model space represent approximately 97% of the complete-space $N_{\text{max}} = 12$ binding energy in the case of ^6Li and reach over 98% for ^6He [Fig. 2 (a) and (b)]. The excitation energies differ only by 5 keV to a few hundred keV from the corresponding complete-space $N_{\text{max}} = 12$ results [see Fig. 2 (c) and (d)], and the agreement with known experimental data is reasonable over a broad range of $\hbar\Omega$ values.

The number of basis states used, e.g., for each ^6Li state, is only about 10-12% for $\langle 2 \rangle 12$, $\langle 4 \rangle 12$, $\langle 6 \rangle 12$, 14% for $\langle 8 \rangle 12$, and 30% for $\langle 10 \rangle 12$ as compared to the num-

TABLE I: Magnetic dipole moments μ [μ_N] and point-particle rms matter radii r_m [fm] of $T = 0$ states of ${}^6\text{Li}$ calculated in the complete $N_{\text{max}} = 12$ space and the $\langle 6 \rangle 12$ subspace for JISP16 and $\hbar\Omega = 20$ MeV. The experimental value for the 1^+ ground-state is known to be $\mu = +0.822 \mu_N$ [40].

		1^+	3^+	2^+	1^+
μ	$N_{\text{max}} = 12$	0.838	1.866	0.970	0.338
	$\langle 6 \rangle 12$	0.839	1.866	1.014	0.338
r_m	$N_{\text{max}} = 12$	2.119	2.063	2.204	2.313
	$\langle 6 \rangle 12$	2.106	2.044	2.180	2.290

ber for the complete $N_{\text{max}} = 12$ model space, which is 3.95×10^6 ($J = 1$), 5.88×10^6 ($J = 2$), and 6.97×10^6 ($J = 3$). The runtime of the SA-NCSM code exhibits a quadratic dependence on the number of $(\lambda\mu)$ and $(S_p S_n S)$ irreps for a nucleus – there are 1.74×10^6 irreps for the complete $N_{\text{max}} = 12$ model space of ${}^6\text{Li}$, while only 8.2%, 8.3%, 8.9%, 12.7%, and 30.6% of these are retained for $N_{\text{max}}^\perp = 2, 4, 6, 8$, and 10, respectively. The net result is that calculations in the $10 \geq N_{\text{max}}^\perp \geq 2$ range require one to two orders of magnitude less time than SA-NCSM calculations for the complete $N_{\text{max}} = 12$ space.

As illustrated in Table I, the magnetic dipole moments obtained in the $\langle 6 \rangle 12$ model space for ${}^6\text{Li}$ agree to within 0.3% for odd- J values, and 5% for $\mu(2_1^+)$. Qualitatively similar agreement is achieved for $\mu(2_1^+)$ of ${}^6\text{He}$, as shown in Table II. The results suggest that it may suffice to

TABLE II: Selected observables for the two lowest-lying states of ${}^6\text{He}$ obtained in the complete $N_{\text{max}} = 12$ space and $\langle 8 \rangle 12$ model subspace for JISP16 and $\hbar\Omega = 20$ MeV.

	$N_{\text{max}} = 12$	$\langle 8 \rangle 12$
$B(E2; 2_1^+ \rightarrow 0_1^+)$ [$e^2\text{fm}^4$]	0.181	0.184
$Q(2_1^+)$ [efm^2]	-0.690	-0.711
$\mu(2_1^+)$ [μ_N]	-0.873	-0.817
$r_m(2_1^+)$ [fm]	2.153	2.141
$r_m(0_1^+)$ [fm]	2.113	2.110

include all low-lying $\hbar\Omega$ states up to a fixed limit, e.g. $N_{\text{max}}^\perp = 6$ for ${}^6\text{Li}$ and $N_{\text{max}}^\perp = 8$ for ${}^6\text{He}$, to account for the most important correlations that contribute to the magnetic dipole moment.

To explore how close one comes to reproducing the important long-range correlations, we compared observables that are sensitive to the tails of the wavefunctions; specifically, the point-particle root-mean-square (rms) matter radii, the electric quadrupole moments and the reduced electromagnetic $B(E2)$ transition strengths that could hint at rotational features [41]. As Table II shows, the complete-space $N_{\text{max}} = 12$ results for these observables are remarkably well reproduced by the SA-NCSM for ${}^6\text{He}$ in the restricted $\langle 8 \rangle 12$ space. In addition, the results for the rms matter radii of ${}^6\text{Li}$, listed in Table I, agree to within 1% for the $\langle 6 \rangle 12$ model space.

Notably, the $\langle 2 \rangle 12$ eigensolutions for ${}^6\text{Li}$ yield results for $B(E2)$ strengths and quadrupole moments that track closely with their complete $N_{\text{max}} = 12$ space counterparts (see Fig. 3). It is known that further expansion of the model space beyond $N_{\text{max}} = 12$ is needed to reach convergence [42, 43]. However, the close correlation between the $N_{\text{max}} = 12$ and $\langle 2 \rangle 12$ results is strongly suggestive that this convergence can be obtained through the leading SU(3) irreps in a symmetry-adapted space. In addition, the results [Fig. 3 (c)] reproduce the ground-state quadrupole moment [39] that is measured to be $Q(1^+) = -0.0818(17) \text{efm}^2$ [40].

The differences between truncated-space and complete-space results are found to be essentially $\hbar\Omega$ insensitive and appear sufficiently small as to be nearly inconsequential relative to the dependences on $\hbar\Omega$ and on N_{max} [see Fig. 3 (b) and (d)]. Since the NN interaction dominates contributions from three-nucleon forces (3NFs) in light nuclei, except for selected cases [5–7], we expect our results to be robust and carry forward to planned applications that will include 3NFs.

To summarize, the results reported in this paper demonstrate that observed collective phenomena in light nuclei emerge naturally from first-principle considerations. This is illustrated through detailed calculations in a SA-NCSM framework for ${}^6\text{Li}$, ${}^6\text{He}$, and ${}^8\text{Be}$ nuclei using the JISP16 and chiral N^3LO NN realistic interactions. The results underscore the strong dominance

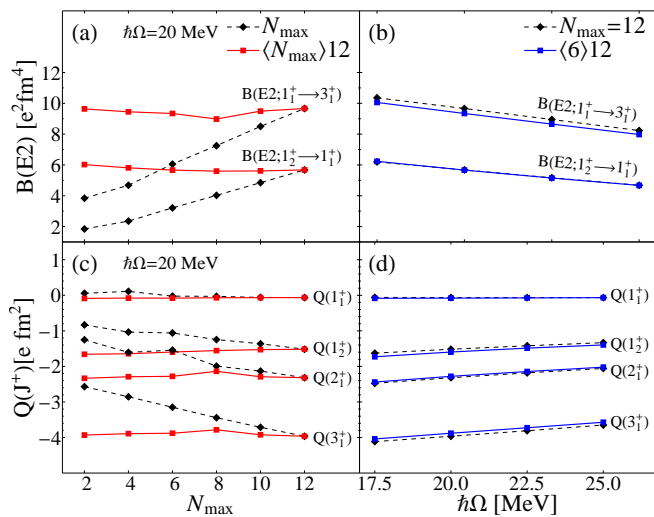


FIG. 3: Electric quadrupole transition probabilities and quadrupole moments for $T = 0$ states of ${}^6\text{Li}$ calculated using the JISP16 interaction without using effective charges are shown for the complete N_{max} (dashed black lines) and truncated $\langle N_{\text{max}}^\perp = N_{\text{max}} \rangle 12$ (solid red lines) model spaces [(a) and (c)], and as a function of $\hbar\Omega$ for the complete $N_{\text{max}} = 12$ space and $\langle 6 \rangle 12$ truncated space (solid blue lines) [(b) and (d)]. Experimentally, $B(E2; 1_1^+ \rightarrow 3_1^+) = 25.6(20) e^2\text{fm}^4$ [40].

of configurations with large deformation and low spins. The results also suggest a path forward to include higher-lying correlations that are essential to collective features such as enhanced B(E2) transition strengths. The results further anticipate the significance of LS -coupling and SU(3) as well as an underlying symplectic symmetry for an extension of *ab initio* methods to the heavier, strongly deformed nuclei of the lower ds shell, and, perhaps, even reaching beyond.

We thank David Rowe and Andrey Shirokov for useful discussions. This work was supported in part by the US NSF [OCI-0904874, OCI-0904809, PHY-0904782], the US Department of Energy [DESC0008485, DE-FG02-95ER-40934, DE-FG02-87ER40371], the National Energy Research Scientific Computing Center [supported by DOE's Office of Science under Contract No. DE-AC02-05CH1123], the Southeastern Universities Research Association, and by the Research Corporation for Science Advancement under a Cottrell Scholar Award. This work also benefitted from computing resources provided by the Louisiana Optical Network Initiative and Louisiana State University's Center for Computation & Technology. T. D. and D. L. acknowledge support from Michal Pajr and CQK Holding.

-
- [1] P. Sternberg, E. G. Ng, C. Yang, P. Maris, J. P. Vary, M. Sosonkina and H. V. Le, In Proc. 2008 ACM/IEEE Conf. on Supercomputing, Austin, November 2008, IEEE Press, Piscataway, NJ, 15:1 (2008).
- [2] P. Maris, M. Sosonkina, J. P. Vary, E. G. Ng and C. Yang, ICCS 2010, Procedia Computer Science **1**, 97(2010).
- [3] H. M. Aktulga, C. Yang, E. N. Ng, P. Maris and J. P. Vary, Euro-par 2012, Lecture Notes on Computer Science **7484**, 830 (2012).
- [4] P. Navrátil, J. P. Vary and B. R. Barrett, *Phys. Rev. Lett.* **84**, 5728 (2000); *Phys. Rev. C* **62**, 054311 (2000).
- [5] B.R. Barrett, P. Navrátil and J.P. Vary, *Prog. Part. Nucl. Phys.* **69**, 131 (2013).
- [6] P. Maris, J. P. Vary, P. Navrátil, W. E. Ormand, H. Nam and D. J. Dean, *Phys. Rev. Lett.* **106**, 202502 (2011).
- [7] P. Maris, J. P. Vary and P. Navrátil, *Phys. Rev. C* **87**, 014327 (2013).
- [8] R. B. Wiringa and S. C. Pieper, *Phys. Rev. Lett.* **89**, 182501 (2002).
- [9] G. Hagen, T. Papenbrock, D. J. Dean and M. Hjorth-Jensen, *Phys. Rev. Lett.* **101**, 092502 (2008).
- [10] T. Neff and H. Feldmeier, *Nucl. Phys. A* **738** (2004) 357.
- [11] S. Quaglioni and P. Navrátil, *Phys. Rev. Lett.* **101**, 092501 (2008).
- [12] S. K. Bogner, R. J. Furnstahl, P. Maris, R. J. Perry, A. Schwenk and J. P. Vary, *Nucl. Phys. A* **801**, 21 (2008).
- [13] R. Roth, J. Langhammer, A. Calci, S. Binder and P. Navrátil, *Phys. Rev. Lett.* **107**, 072501 (2011).
- [14] E. Epelbaum, H. Krebs, D. Lee and U.-G. Meissner, *Phys. Rev. Lett.* **106**, 192501 (2011); E. Epelbaum, H. Krebs, T. A. Lähde, D. Lee, U.-G. Meissner, *Phys. Rev. Lett.* **109**, 252501 (2012).
- [15] P. Maris, A. M. Shirokov and J. P. Vary, *Phys. Rev. C* **81**, 021301(R) (2010).
- [16] V.Z. Goldberg et al., *Phys. Lett. B* **692**, 307 (2010)
- [17] B. Davids, R. H. Cyburt, J. Jose and S. Mythili, *Astrophys. J.* **735**, 40 (2011).
- [18] A. M. Laird et al., *Phys. Rev. Lett.* **110**, 032502 (2013).
- [19] A. M. Shirokov, J. P. Vary, A. I. Mazur and T. A. Weber, *Phys. Letts. B* **644**, 33 (2007).
- [20] D. R. Entem and R. Machleidt, *Phys. Rev. C* **68**, 041001 (2003).
- [21] J. P. Elliott, *Proc. Roy. Soc. A* **245**, 128 (1958).
- [22] J. P. Draayer, T. Dytrych, K. D. Launey and D. Langr, *Prog. Part. Nucl. Phys.* **67**, 516 (2012).
- [23] O. Castaños, J. P. Draayer and Y. Leschber, *Z. Phys* **329**, 33 (1988).
- [24] G. Rosensteel and D. J. Rowe, *Ann. Phys. N.Y.* **104**, 134 (1977).
- [25] Y. Leschber and J. P. Draayer, *Phys. Letts. B* **190**, 1 (1987).
- [26] J. P. Draayer, *Nucl. Phys.* **A216**, 457 (1973).
- [27] N. Anantaraman et al., *Phys. Rev. Lett.* **35**, 1131 (1974).
- [28] J. P. Draayer, *Nucl. Phys.* **A237**, 157 (1975).
- [29] J. P. Draayer, K. J. Weeks and G. Rosensteel, *Nucl. Phys.* **A413**, 215 (1984).
- [30] G. Rosensteel, J. P. Draayer and K. J. Weeks, *Nucl. Phys.* **A419**, 1 (1984).
- [31] J. P. Draayer and K. J. Weeks, *Phys. Rev. Lett.* **51**, 1422 (1983).
- [32] G. Rosensteel and D. J. Rowe, *Phys. Rev. Lett.* **38**, 10 (1977).
- [33] G. Rosensteel and D. J. Rowe, *Ann. Phys. N.Y.* **126**, 343 (1980).
- [34] D. J. Rowe, *Rep. Prog. Phys.* **48**, 1419 (1985).
- [35] D. R. Peterson and K.T. Hecht, *Nucl. Phys.* **344**, 361 (1980).
- [36] T. Dytrych, K. D. Sviratcheva, C. Bahri, J. P. Draayer and J. P. Vary, *Phys. Rev. Lett.* **98**, 162503 (2007).
- [37] B. J. Verhaar, *Nucl. Phys. A* **21**, 508 (1960).
- [38] D. H. Gloeckner and R. D. Lawson, *Phys. Lett. B* **53**, 313 (1974).
- [39] The near vanishing of the quadrupole moment, an L=2 object, in the ground-state of ${}^6\text{Li}$, $Q(1_1^+)$, can be attributed to a very strong dominance ($\sim 87\%$) of L=0 configurations in the ground state.
- [40] D. R. Tilley et al., *Nucl. Phys. A* **708**, 3 (2002).
- [41] M. A. Caprio, P. Maris and J. P. Vary, *Phys. Lett. B* **719**, 179 (2013).
- [42] C. Cockrell, J. P. Vary and P. Maris, *Phys. Rev. C* **86**, 034325 (2012).
- [43] P. Maris and J. P. Vary, *Int. J. Mod. Phys. E* **22**, 1330016 (2013).